Journal of the Physical Society of Japan, Vol. 45, No. 5, November, 1978

Computer Simulation of Temperature and Field Dependences of Sublattice Magnetizations and Spin-Flip Transition in Gallium-Substituted Yttrium Iron Garnet

Noboru Miura, Isamu Oguro and Sōshin Chikazumi

Institute for Solid State Physics, University of Tokyo,
Roppongi, Minato-ku, Tokyo 106

(Received April 28, 1978)

On the basis of the molecular field model, sublattice magnetizations in gallium-substituted yttrium iron garnet $Y_3Ga_xFe_{5-x}O_{12}$ are calculated over a wide range of x, temperature and applied magnetic field with a computer program. Comparing the calculated temperature dependence of spontaneous magnetization, the critical fields of the spin-flip transition at high magnetic fields and the ferrimagnetic Curie temperature, with experimental data, the super-exchange coefficients in YIG and $Y_3Ga_xFe_{5-x}O_{12}$ were evaluated.

§1. Introduction

The ferrimagnetic iron garnets have been of great interest for many years. They constitute a large class of mixed oxides with the rather complicated cubic structure. Yttrium iron garnet (YIG) is the simplest magnetic member of this series, since it consists of only two magnetic sublattices formed with Fe^{3+} ions. The chemical formula of YIG is conveniently written as $\{Y_3\}[Fe_2](Fe_3)O_{12}$. In each formula unit, there are three Fe^{3+} ions in tetrahedral sites (24(d) positions; hereafter referred to as d-site) and two Fe^{3+} ions in octahedral sites (16(a) positions; hereafter referred to as a-site). The super-exchange interaction coefficient J_{ad} between Fe^{3+} ions at a- and d-sites is negative (antiferromagnetic), and a net magnetization is produced in the direction of the d-site moment. The intrasite super-exchange coefficients J_{aa} and J_{dd} are also known to be negative.

The values of the exchange coefficients J_{aa}, J_{dd} and J_{ad} have been reported by many authors as listed in Table I. There have been considerable discrepancies among these data, particularly for J_{aa} and J_{dd}. Anderson analysed the spontaneous magnetization vs temperature curve based on the molecular field model.[6] Unfortunately, however, such a temperature dependence of spontaneous magnetization curve, or a thermomagnetic curve is not so sensitive to the exact values of the exchange coefficients, so that it has been difficult to

Table I. Exchange coefficients in YIG.

Year	Authors	$-J_{aa}$	$-J_{dd}$ (cm^{-1})	$-J_{ad}$	Ref.
1958	Pauthenet	5.74	10.29	24.19	1
1960	Aleonard	6.1	10.3	25.2	2
1962	Wojtowicz	0	0	24.3	3
1963	Boyd *et al.*	0	0	13.6	4
1963	Harris	6.35	6.35	31.8	5
1964	Anderson (set A)	8.45	11.86	25.36	6
	(set C)	7.8	11.0	25.36	
	(set B)	0	0	13.61	
1966	Lüthi	1.04	1.39	22.9	16
1967	Harris	0.2	2.5	24.6	7
1967	Gonano *et al.*	0.5	2.0	22.5	8
1976	Guillot and Gall	0	0	14	9

obtain a unique set of exchange coefficients with high accuracy from such a thermomagnetic curve.

When a ferrimagnetic material is subjected to high magnetic fields comparable to the exchange field, its spin structure is expected to be radically altered. The magnetic field induced spin-flip transition has been observed in several rare earth iron garnets.[11] In rare earth iron garnets which have compensation points T_c, the critical field for the spin-flip transition becomes low near T_c. The critical field is very sensitive to the value of the intersite exchange coefficient. Therefore, the measurement of the spin-flip transition is a useful means to determine the exchange coefficients. The molecular field arising from the exchange interactions in YIG is of the order of several megagauss. Recently, techniques have been developed for generating the ultrahigh magnetic field in the megagauss range,[11] which open up a possibility to observe the spin-flip transition in substances with such large exchange fields as YIG.

The large exchange fields in YIG can be reduced by substitution of nonmagnetic ions for Fe^{3+} ion. Many investigations have been made on the magnetization of gallium substituted YIG, $Y_3Ga_xFe_{5-x}O_{12}$.[12-18] When Ga^{3+} ions are substituted for Fe^{3+}, Ga^{3+} is known to substitute preferentially onto the d-site. For small x ($x \lesssim 2$), the net magnetization of $Y_3Ga_xFe_{5-x}O_{12}$ decreases almost linearly with x, and it crosses zero at about $x=1.25$.[14] Depending on x, the spontaneous magnetization exhibits various types of temperature dependence of ferrimagnets in the Néel's theory (R-, Q-, P-, or N-types).[19,20] Recently, the spin-flip transition was observed in the measurement of the Faraday rotation on $Y_3Ga_xFe_{5-x}O_{12}$ ($x=0.5$, 1.0) at very high magnetic fields up to 2 MG.[11] Because of its rather simple sublattice structure despite the complex crystal structure, $Y_3Ga_xFe_{5-x}O_{12}$ provides a good system for investigating temperature dependence and magnetic field dependence of the sublattice magnetization in a ferrimagnet.

In this paper, we study the temperature and field dependences of sublattice magnetizations and the spin-flip transition in $Y_3Ga_xFe_{5-x}O_{12}$, based on the molecular field model. The calculation was performed for arbitrary x, temperature and applied magnetic field, with a computer program. In order to discuss the exchange coefficients for YIG, the calculated results are compared with experiments of the magnetization and the Faraday rotation.

§2. Magnetization in Zero Applied Field

The molecular fields $\boldsymbol{H}_a$ and $\boldsymbol{H}_d$ acting on the two sublattice sites in $Y_3Ga_xFe_{5-x}O_{12}$ are expressed as

$$\boldsymbol{H}_a = \boldsymbol{H}_0 + n_{aa}\boldsymbol{M}_a + n_{ad}\boldsymbol{M}_d, \qquad (2.1)$$

$$\boldsymbol{H}_d = \boldsymbol{H}_0 + n_{ad}\boldsymbol{M}_a + n_{dd}\boldsymbol{M}_d, \qquad (2.2)$$

where $\boldsymbol{H}_0$ is the external magnetic field, n_{ij} are the molecular field coefficients, and $\boldsymbol{M}_a$ and $\boldsymbol{M}_d$ are the sublattice magnetizations per unit volume for the a- and d-sites, respectively. The coefficients n_{ij} are related to the exchange coefficients by

$$n_{ad} = n_{da} = \frac{2Z_{ad}J_{ad}}{\mu N(g\mu_B)^2} = \frac{2Z_{da}J_{ad}}{\lambda N(g\mu_B)^2}, \qquad (2.3)$$

$$n_{aa} = \frac{2Z_{aa}J_{aa}}{\lambda N(g\mu_B)^2}, \qquad (2.4)$$

$$n_{dd} = \frac{2Z_{dd}J_{dd}}{\mu N(g\mu_B)^2}, \qquad (2.5)$$

where μ_B is the Bohr magneton, Z_{ij} are the numbers of the nearest neighbor j-site ions surrounding an i-site ion, N is the number of Fe^{3+} ions per unit volume, and λ and μ represent the fraction of the Fe^{3+} ions in the a- and d-sites, respectively.

Starting from (2.1) and (2.2) the spontaneous magnetization of YIG can be calculated putting $H_0=0$, along with the molecular field theory described in the Appendix, once the exchange coefficients J_{ij} are given. For YIG, numbers of nearest neighbors Z_{ij} are:

$$Z_{aa}=8 \quad Z_{ad}=6 \quad Z_{da}=4, \quad Z_{dd}=4,$$

and other quantities are as follows:

$$\lambda=0.4, \quad \mu=0.6, \quad S=\frac{5}{2}, \quad g=2.$$

The data of J_{ij} listed in Table I are in poor agreement with each other. The ferrimagnetic Curie temperature Θ_f of YIG is 559 K.[6] Few sets of the coefficients in Table I give the experimental value of $\Theta_f=559$ K when put into (A·8). If we assume that $J_{aa}=J_{dd}=0$, we obtain $J_{ad}=13.61$ cm^{-1} (Anderson's set B)[6] in order to satisfy $\Theta_f=559$ K. This is a set of values of an extreme case where a-a and d-d interactions are absent. The other two sets of coefficients given by Anderson[6] also lead to $\Theta_f=559$ K. The set A assumes relatively large values of J_{aa} and J_{dd} contrary to the set B, and it is another set of contrasting extreme case.

Figure 1 shows temperature dependence of the spontaneous magnetization of YIG calculated assuming two different sets of J_{ij} (Anderson's set A and B). Although the differences in the assumed values of J_{ij} are fairly large between the two sets, there is only little difference in the shape of the thermomagnetic curve. Consequently, it is difficult to obtain a unique set of interaction coefficients only from such a thermomagnetic curve for YIG.

The magnetization for gallium substituted YIG, $Y_3Ga_xFe_{5-x}O_{12}$ can also be calculated in a similar way. We rewrite the chemical formula as $Y_3[Ga_yFe_{2-y}](Ga_zFe_{3-z})O_{12}$, where $x=y+z$; the ions in a-site are enclosed by square brackets and those in d-site by curved brackets. The fraction of Ga^{3+} ions in d-site i.e. $f_t=z/x$ was evaluated by Geller *et al.* as a function of x. The dependence of $2-y$ and $3-z$ on x are reproduced in Fig. 2 from ref. 14. We see that the Ga^{3+} ion has a greater preference for d-site than for a-site.

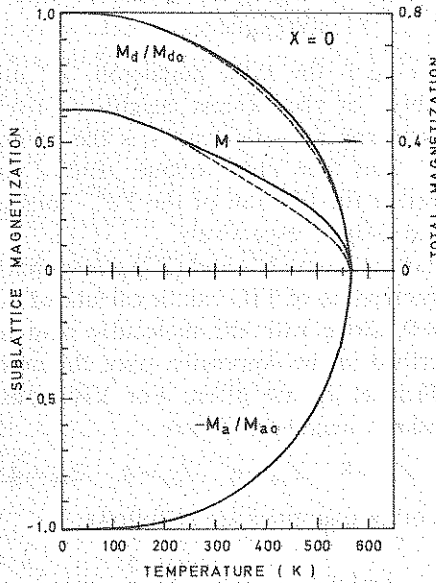

Fig. 1. Spontaneous magnetization and sublattice magnetizations of YIG. The total magnetization is plotted in units of $Ng\mu_B$. The solid curves are calculated with $J_{aa}=-8.45$ cm^{-1}, $J_{dd}=-11.86$ cm^{-1} and $J_{ad}=-25.36$ cm^{-1} (set A), and the broken curves with $J_{aa}=J_{dd}=0$, $J_{ad}=13.61$ cm^{-1} (set B).

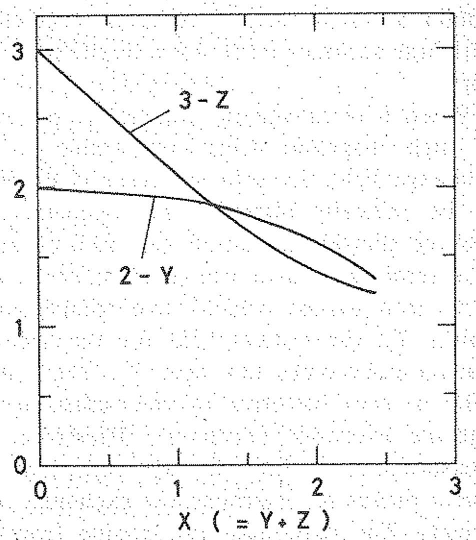

Fig. 2. Fraction of Fe^{3+} ion in each sub-lattice site of $Y_3Ga_xFe_{5-x}O_{12}$ as a function of x. The curves were calculated from the data in ref. 12.

For gallium substituted YIG, we can express Z_{ij}, λ and μ as follows:

$$
\begin{aligned}
&Z_{aa}=8\times(2-y)/2, \quad Z_{ad}=6\times(3-z)/3,\\
&Z_{da}=4\times(2-y)/2, \quad Z_{dd}=4\times(3-z)/3,\\
&\lambda=0.4\times(2-y)/2, \quad \mu=0.6\times(3-z)/3. \qquad (2.6)
\end{aligned}
$$

For small x, we may assume that J_{ij} do not change with x, that is, J_{ij} are independent of gallium substitution. Within this approximation, it follows that n_{ij} are also independent of x from (2.3)~(2.5). The calculated magnetization curves for $x=0.5$, $x=1.0$ and $x=1.5$ are shown in Fig. 3(a), (b) and (c), respectively. Here Anderson's set A of the exchange coefficients were assumed. As is seen in the figures, the shape of the magnetization curve changes drastically with a small increase of x; i.e. curves of R-type for $x=0$, Q-type for $x=0.5$, P-type for $x=1.0$ and N-type for $x=1.5$ appear successively. Such a change in the thermomagnetic curve shape has actually been observed in experiments.[16,23] On the other hand, if we assume that the intrasite interactions are absent as in the set

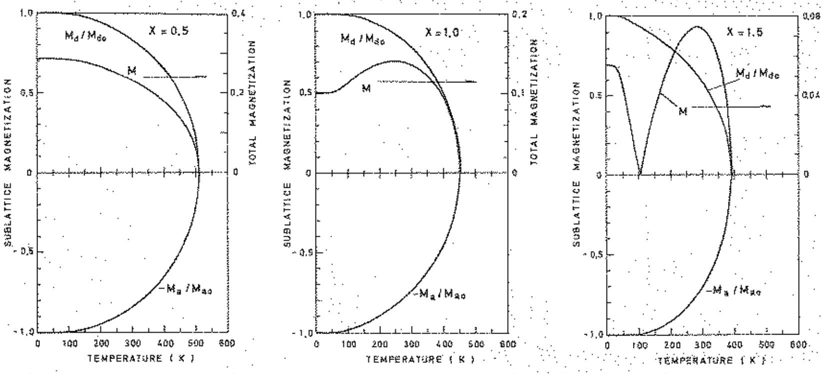

(a) (b) (c)

Fig. 3. Spontaneous magnetization and sublattice magnetizations of $Y_3Ga_xFe_{5-x}O_{12}$ for (a) $x=0.5$ (b) $x=1.0$ and (c) $x=1.5$. The total magnetization is plotted in a unit of $Ng\mu_B$. The calculations were made with the parameter set A.

B, the curve shape should be always R-type irrespective of x and the above mentioned change should not appear. Accordingly, we can deduce qualitatively that there are significant contributions of the a-a and d-d interactions to the magnetization of $Y_3Ga_xFe_{5-x}O_{12}$.

§3. Spin-Flip Transition

Sublattice magnetizations and the spin-flip transition of ferrimagnets in high mangetic fields have been discussed by several authors.[21,22] In this section, we shall concentrate on the spin-flip transition of $Y_3Ga_xFe_{5-x}O_{12}$. As is shown in Fig. 4, when the applied field H_0 is lower than a threshold H_{c1} (region I), two sublattice magnetizations $\boldsymbol{M}_a$ and $\boldsymbol{M}_d$ remain collinear and the crystal exhibits usual ferrimagnetic properties. Since the moment $\boldsymbol{M}_a$ is along the opposite direction to $\boldsymbol{H}_0$ in this configuration, when H_0 becomes high enough, $\boldsymbol{M}_a$ may rotate towards the direction of $\boldsymbol{H}_0$ in spite of the oppositely directed effective field coming from the interaction with $\boldsymbol{M}_d$. If $\boldsymbol{M}_a$ changes its direction, the vector $\boldsymbol{M}_d$ may also be influenced by the exchange interaction between $\boldsymbol{M}_a$ and $\boldsymbol{M}_d$. In this way, when H_0 exceeds a certain critical field H_{c1}, noncollinear phase (spin cant phase) occurs as the region II in Fig. 4. As the field increases further in the canted configuration, the angle between vectors $\boldsymbol{M}_a$ and $\boldsymbol{M}_d$ decreases. Finally when H_0 exceeds the second critical field H_{c2} (region III), the system enters a collinear phase again, where both $\boldsymbol{M}_a$ and $\boldsymbol{M}_d$ are in the same direction with $\boldsymbol{H}_0$. This is the field induced spin-flip transition in a two-sublattice ferrimagnet.

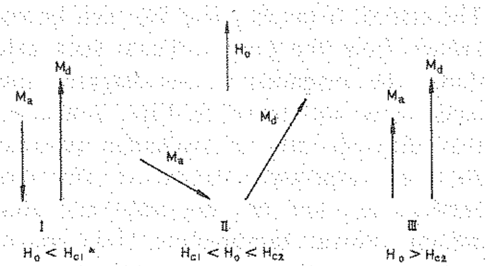

Fig. 4. Sublattice magnetizations in external magnetic fields. Regions I and III are the collinear phase and II is the spin cant phase.

The critical fields H_{c1} and H_{c2} can be obtained using the molecular field relations (2.1) and (2.2). In the following argument, we shall neglect effects of the magnetic anisotropy. Eliminating $\boldsymbol{H}_0$ from (2.1) and (2.2), we have

$$\boldsymbol{H}_a-(n_{aa}-n_{ad})\boldsymbol{M}_a=\boldsymbol{H}_d-(n_{dd}-n_{ad})\boldsymbol{M}_d. \quad (3.1)$$

As the sublattice magnetizations lie along their molecular field, it is required that $\boldsymbol{M}_a//\boldsymbol{H}_a$ and $\boldsymbol{M}_d//\boldsymbol{H}_d$. Equation (3.1) is a general relationship which should hold for all the the configurations in Fig. 4. In the spin cant phase, $\boldsymbol{M}_a$ and $\boldsymbol{M}_d$ are not parallel with each other. Therefore, (3.1) requires that the both sides of (3.1) should be zero in the cant phase:

$$\boldsymbol{H}_a=(n_{aa}-n_{ad})\boldsymbol{M}_a, \quad (3.2)$$

$$\boldsymbol{H}_d=(n_{dd}-n_{ad})\boldsymbol{M}_d. \quad (3.3)$$

Inserting these into (2.1) or (2.2), we obtain

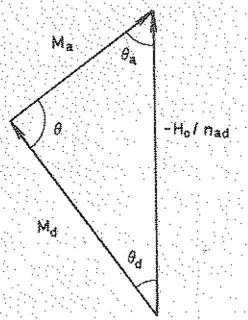

Fig. 5. Relationship between vectors $\boldsymbol{M}_a$, $\boldsymbol{M}_d$ and $\boldsymbol{H}_0/(-n_{ad})$. A triangle is formed with the three vectors. Angles θ_a, θ_d and θ are defined as shown in the figure.

$$\boldsymbol{M}_a+\boldsymbol{M}_d=\boldsymbol{H}_0/(-n_{ad}). \qquad (3.4)$$

The relation (3.4) means that the vectors $\boldsymbol{M}_a$, $\boldsymbol{M}_d$ and $\boldsymbol{H}_0/(-n_{ad})$ form a triangle as is shown in Fig. 5. A necessary condition for these vectors to form a triangle is

$$|M_d-M_a|<H_0/(-n_{ad})<M_a+M_d. \qquad (3.5)$$

In another words, the lower and the upper critical fields of the spin cant phase are given by

$$H_{c1}=-n_{ad}|M_d-M_a|, \qquad (3.6)$$

$$H_{c2}=-n_{ad}(M_a+M_d). \qquad (3.7)$$

Some other important properties of the spin cant phase are also led from the above argument. Equations (3.2) and (3.3) show that the molecular field acting on $\boldsymbol{M}_a$ and $\boldsymbol{M}_d$ are determined only by $\boldsymbol{M}_a$ and $\boldsymbol{M}_d$ themselves and are independent of $\boldsymbol{H}_0$. This means that magnitudes of the sublattice magnetizations $\boldsymbol{M}_a$ and $\boldsymbol{M}_d$ are independent of the external field in the whole region of the spin cant phase. Moreover, $\boldsymbol{M}_a$ and $\boldsymbol{M}_d$ can be calculated as if each of them were the spontaneous magnetization of a simple ferromagnetic substance with a new molecular field coefficient ($n_{aa}-n_{ad}$ or $n_{dd}-n_{ad}$).

It is also an important point that the total magnetization $\boldsymbol{M}=\boldsymbol{M}_a+\boldsymbol{M}_d$ equals to $\boldsymbol{H}_0/(-n_{ad})$ and is independent of temperature. These properties mentioned above simplify the calculation of the magnetizations for the spin cant phase.

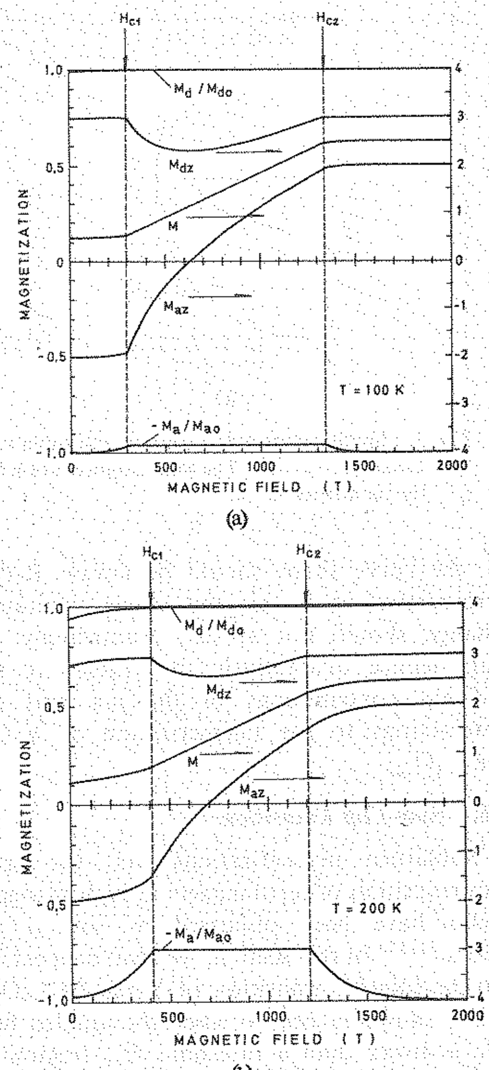

(a)

(b)

Fig. 6. Magnetic field dependence of M, M_a, M_{az}, M_d and M_{dz} in YIG. The calculations were performed with set A. M_{az} and M_{dz} are plotted in units of $N/5g\mu_B$, and M is in units of $2/5Ng\mu_B$. Temperature is (a) 100 K (b) 200 K.

Examples of the field dependence of the sublattice magnetizations and the total magnetization in YIG at constant temperatures are shown in Fig. 6 for the parameter set A. The critical fields H_{c1} and H_{c2} can be readily known from the graphs. From such calculations, the magnetic phase diagram can be constructed as shown in Figs. 7 and 8, for two different sets of exchange parameters. As the temperature is raised, the interval between H_{c1} and H_{c2} decreases and above a certain critical temperature, the spin cant phase does not occur any more. The broken curves in Figs. 7 and 8 represent the boundary between the antiparallel collinear (ferrimag-

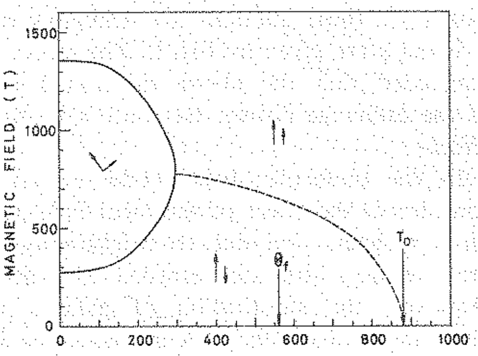

Fig. 7. Magnetic phase diagram of YIG assuming the parameter set A ($J_{aa}=-8.45$ cm^{-1}, $J_{dd}=-11.86$ cm^{-1}, $J_{ad}=-25.36$ cm^{-1}).

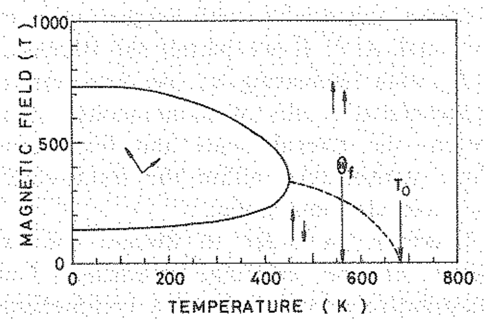

Fig. 8. Magnetic phase diagram of YIG assuming the parameter set B ($J_{aa}=J_{dd}=0$, $J_{ad}=-13.61$ cm^{-1}).

netic) and the parallel collinear (paramagnetic) phase. On this curve, $M_a=0$. This leads to

$$H_d=(n_{dd}-n_{ad})M_d, \tag{3.8}$$

the same equation as (3.3). It should be noted that this broken curve crosses the abscissa at a much higher temperature T_0 than the ferrimagnetic Curie temperature Θ_f. This shows that the ferrimagnetic order arises at an infinitesimally small external field even above Θ_f.

If we compare Figs. 7 and 8, we can see that the critical fields for the spin-flip transition are very sensitive to the choice of the values of the exchange coefficients. Assuming the parameter set A, the critical field H_{c1} of YIG is very high as in Fig. 7. Substitution of Ga^{3+} for Fe^{3+} reduces the critical fields. The magnetic phase diagram for $Y_3Ga_xFe_{5-x}O_{12}$ can be calculated similarly by modifying the parameters as described in §2. Results of calculation of H_{c1} are shown in Fig. 9 as a function of temperature for various x. With increasing

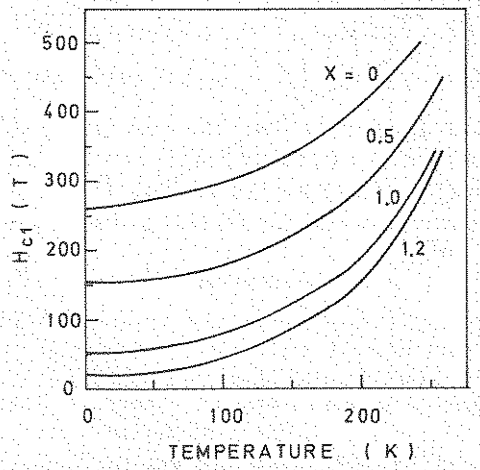

Fig. 9. Dependence of H_{c1} on T. The set A was assumed in the calculation.

x, H_{c1} decreases significantly, and H_{c1} at $T=0$ should become zero for about $x=1.25$.

§4. Discussion

As is shown in Figs. 1 and 3, $Y_3Ga_xFe_{5-x}O_{12}$ exhibits various types of temperature dependence of the spontaneous magnetization with varying x. This characteristic was actually observed experimentally in $Y_3Ga_xFe_{5-x}O_{12}$ for various x.[16,23] It should be noted at his point that the curves in Fig. 3 were obtained assuming finite intrasite exchange coefficients (set A). If we assume, on the other hand, that the intrasite exchange coefficients are zero (set B), the curves should be R-type for the whole range of x. This fact implies that the intrasite interaction should be of a considerable amount.

On the other hand, the set A results in much higher critical fields of the spin-flip transition than the set B. (Figs. 7 and 8). In the recent experiment of the Faraday rotation in $Y_3Ga_xFe_{5-x}O_{12}$ at very high magnetic fields, it was found that H_{c1} is much lower than expected from the set A for $x=0.5$ and $x=1.0$.[11] The experimental points were closer to the curves calculated with set B, but the experimentally observed temperature dependence of H_{c1} is larger than the calculation with set A. Although there are some ambiguity in the estimation of x in this experiment, the experimental results show that the exchange coefficient $-J_{ad}$ in gallium substituted YIG should be somewhat smaller than in pure

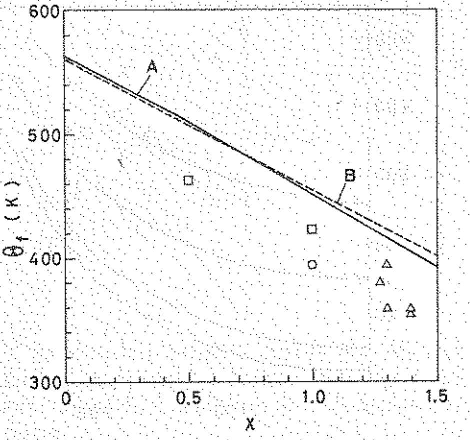

Fig. 10. Dependence of Θ_f on x. The solid and broken curves were calculated with parameter set A and B, respectively. Experimental points are plotted for the present experiment (○—samples from Bell Laboratories, □—samples from National Institute for Researches in Inorganic Materials) and the data of Lüthi (△, ref. 16).

YIG as far as we assume the set A for YIG.

Figure 10 is a plot of the variation of the ferrimagnetic Curie temperature as a function of x.[23] Theoretical lines were calculated along with the treatment in §2 with parameters of the set A and B. Although there is a scatter of the experimental points, it is noted that the theoretical curves give higher Θ_f than the experiments. This means also that $-J_{ad}$ for $x \neq 0$ should be smaller than assumed in §2.

We have assumed in §2 that the exchange coefficients $-J_{ij}$ for $Y_3Ga_xFe_{5-x}O_{12}$ does not change with x. However, there might be a possibility that it decreases with increasing x. Gilleo considered the variation of magnetic moment and ferrimagnetic Curie temperature in terms of the change in the number of active exchange linkages per magnetic ion.[24] Magnetic ions which interact with no other magnetic ions or with only one other magnetic ion in another site cannot be active in a cooperative interaction with the remainder of the ions, so that those ions must be excluded from participation in ferrimagnetism. According to Gilleo,[24] the probability that an ion in a- or d-site be linked with none or at most one of the magnetic ions in another site is given by

$$E_a = 6(z/3)^5 - 5(z/3)^6, \tag{4.1}$$

$$E_d = 4(y/2)^3 - 3(y/2)^4. \tag{4.2}$$

For $x \lesssim 2$, these fractions are negligibly small if y and s are given by Fig. 2. Therefore, it is concluded that the above mentioned break of the exchange linkage has only a negligible effect.

In the molecular field model so far we considered, the effect of the local field acting on a magnetic ion due to neighboring ions are averaged and are regarded as uniform. However, the substitution of gallium may alter the environment of a magnetic ion in a different way from that considered in the molecular field model in §2. Accordingly, there is a good reason to consider that the molecular field coefficient $-n_{ij}$ or $-J_{ij}$ might decrease appreciably with increasing x even for small x.[11] If we permit the decrease of $-J_{ij}$ with increasing x, we can interpret experimental results of spontaneous magnetization, the critical fields and ferrimagnetic Curie temperature within the framework of the molecular field model.

However, in order to discuss the exact values of the exchange coefficients more quantitatively, we need more comprehensive experimental results for the above quantities on crystals of which y and z are accurately known.

Appendix: Molecular Field Model for a Two-Sublattice Ferrimagnet

If we designate the thermally averaged value of the spins of ions in the a- and d-site in the direction of each sublattice magnetization as $\langle S_a \rangle$ and $\langle S_d \rangle$, the sublattice magnetizations are expressed in terms of $\langle S_a \rangle$ and $\langle S_d \rangle$:

$$M_a = \lambda N g \mu_B \langle S_a \rangle, \tag{A·1}$$

$$M_d = \mu N g \mu_B \langle S_d \rangle. \tag{A·2}$$

Putting (A·1) and (A·2) into (2.1) and (2.2), we have,

$$H_a = H_0 + \frac{2Z_{aa}J_{aa}}{g\mu_B}\langle S_a \rangle + \frac{2Z_{ad}J_{ad}}{g\mu_B}\langle S_d \rangle, \tag{A·3}$$

$$H_d = H_0 + \frac{2Z_{dd}J_{dd}}{g\mu_B}\langle S_d \rangle + \frac{2Z_{ad}J_{ad}}{g\mu_B}\langle S_a \rangle. \tag{A·4}$$

Magnitudes of $\langle S_a \rangle$ and $\langle S_d \rangle$ are given by

$$\langle S_a \rangle = S_{ao} B_{S_{ao}}\left(\frac{g\mu_B H_a S_{ao}}{k_B T}\right), \tag{A·5}$$

$$\langle S_\mathrm{d}\rangle = S_\mathrm{do}\mathrm{B}_{S_\mathrm{do}}\left(\frac{g\mu_\mathrm{B}H_\mathrm{d}S_\mathrm{do}}{k_\mathrm{B}T}\right), \qquad (\mathrm{A}\cdot 6)$$

where $\mathrm{B}_s(x)$ is the Brillouin function and S_ao and S_do are the values of $\langle S_\mathrm{a}\rangle$ and $\langle S_\mathrm{d}\rangle$ at $T=0$. Combining (A·3)–(A·6), $\langle S_\mathrm{a}\rangle$ and $\langle S_\mathrm{d}\rangle$ can be numerically calculated.

In the collinear phase, the total magnetization is

$$M = M_\mathrm{d} \mp M_\mathrm{a} = Ng\mu_\mathrm{B}[\mu\langle S_\mathrm{d}\rangle \mp \lambda\langle S_\mathrm{a}\rangle]. \qquad (\mathrm{A}\cdot 7)$$

The minus and plus signs are for the antiparallel and parallel phase, respectively. The ferrimagnetic Curie temperature is given by$^{20)}$

$$\Theta_f = S(S+1)/3k_\mathrm{B}\cdot\left[Z_\mathrm{aa}J_\mathrm{aa} + Z_\mathrm{dd}J_\mathrm{dd} + \sqrt{(Z_\mathrm{aa}J_\mathrm{aa} - Z_\mathrm{dd}J_\mathrm{dd})^2 + 4(\lambda/\mu)Z_\mathrm{ad}^2J_\mathrm{ad}^2}\,\right], \qquad (\mathrm{A}\cdot 8)$$

where $S = S_\mathrm{ao} = S_\mathrm{do} = 5/2$, and k_B is the Boltzmann constant.

When the applied field H_0 satisfies (3.5), the spin cant phase occurs, where the triangle relation holds as in Fig. 6. In this configuration the projection of each sublattice magnetization in the direction of the external field is given by

$$M_\mathrm{az} = M_\mathrm{a}\cos\theta_\mathrm{a}, \qquad (\mathrm{A}\cdot 9)$$

$$M_\mathrm{dz} = M_\mathrm{d}\cos\theta_\mathrm{d}, \qquad (\mathrm{A}\cdot 10)$$

where

$$\cos\theta_\mathrm{a} = [M_\mathrm{a}^2 + (H_0/n_\mathrm{ad})^2 - M_\mathrm{d}^2]/[2\cdot M_\mathrm{a}H_0/(-n_\mathrm{ad})],$$
$$\cos\theta_\mathrm{d} = [M_\mathrm{d}^2 + (H_0/n_\mathrm{ad})^2 - M_\mathrm{a}^2]/[2\cdot M_\mathrm{d}H_0/(-n_\mathrm{ad})]. \qquad (\mathrm{A}\cdot 11)$$

The total magnetization is expressed as

$$M = M_\mathrm{az} + M_\mathrm{dz} = H_0/(-n_\mathrm{ad}), \qquad (\mathrm{A}\cdot 12)$$

which is consistent with (3.4). The molecular fields are

$$H_\mathrm{a} = H_0\cos\theta_\mathrm{a} + n_\mathrm{aa}M_\mathrm{a} - n_\mathrm{ad}M_\mathrm{d}\cos\theta, \qquad (\mathrm{A}\cdot 13)$$

$$H_\mathrm{d} = H_0\cos\theta_\mathrm{d} + n_\mathrm{dd}M_\mathrm{d} - n_\mathrm{ad}M_\mathrm{a}\cos\theta. \qquad (\mathrm{A}\cdot 14)$$

Since

$$\cos\theta = [M_\mathrm{a}^2 + M_\mathrm{d}^2 - (H_0/n_\mathrm{ad})^2]/(2M_\mathrm{a}M_\mathrm{d}), \qquad (\mathrm{A}\cdot 15)$$

we obtain

$$H_\mathrm{a} = 2/(g\mu_\mathrm{B})(Z_\mathrm{aa}J_\mathrm{aa} - Z_\mathrm{da}J_\mathrm{ad})\langle S_\mathrm{a}\rangle, \qquad (\mathrm{A}\cdot 16)$$

$$H_\mathrm{d} = 2/(g\mu_\mathrm{B})(Z_\mathrm{dd}J_\mathrm{dd} - Z_\mathrm{ad}J_\mathrm{ad})\langle S_\mathrm{d}\rangle. \qquad (\mathrm{A}\cdot 17)$$

These equations can also be derived directly from (3.2) and (3.3). Putting (A·16) and (A·17) into (A·5) and (A·6), sublattice magnetizations are calculated for the spin cant phase.

References

1) R. Pauthenet: Ann. Phys. (France) **3** (1958) 424.
2) R. Aleonard: J. Phys. Chem. Solids **15** (1960) 167.
3) P. J. Wojtowicz: J. appl. Phys. **33** (1962) 1257.
4) E. L. Boyd, V. L. Moruzzi and J. S. Smart: J. appl. Phys. **34** (1963) 3049.
5) A. B. Harris: Phys. Rev. **132** (1963) 2398.
6) E. E. Anderson: Phys. Rev. **134** (1964) A1581.
7) A. B. Harris: Phys. Rev. **155** (1967) 499.
8) R. Gonano, E. Hunt and H. Meyer: Phys. Rev. **156** (1967) 521.
9) M. Guillot and H. Le Gall: Phys. Status solidi (b) **77** (1976) 121.
10) K. P. Belov *et al.*: Soviet Physics-JETP **41** (1976) 590; N. F. Kharchenko, V. V. Eremenko and L. I. Belyi: Soviet Physics-JETP **28** (1969) 219; N. F. Kharchenko, V. V. Eremenko and S. L. Gnatchenko: Soviet Physics-JETP Lett. **20** (1974) 280; R. A. Buchanan and A. E. Clark: Solid State commun. **7** (1969) 1087; N. F. Kharchenko, V. V. Eremenko, S. L. Gnatchenko, L. I. Belyi and É. M. Kabanova: Soviet Physics-JETP **41** (1976) 531; G. Fillon and G. Hug: CR Acad. Sci. (France) **271** (1970) 1045.
11) N. Miura, G. Kido, I. Oguro, K. Kawauchi, S. Chikazumi, J. F. Dillon, Jr. and L. G. Van Uitert: Physica **86–88B** (1977) 1219.
12) M. A. Gilleo and S. Geller: J. appl. Phys. **29** (1958) 380.
13) S. Geller, H. J. Williams, G. P. Espinosa and R. C. Sherwood: The Bell Syst. tech. J. **XLIII** (1964) 565.
14) S. Geller, J. A. Cape, G. P. Espinosa and D. H. Leslie: Phys. Rev. **148** (1966) 522.
15) S. Geller: Z. Krist. **125** (1967) 1.
16) B. Lüthi: Phys. Rev. **148** (1966) 519.
17) H. Mattews, S. Singh and R. C. Le Craw: Appl. Phys. Letters **6** (1965) 165.
18) P. Hansen, P. Röschmann and W. Tolksdorf: J. appl. Phys. **45** (1974) 2728.
19) L. Néel: Ann. Phys. (France) **3** (1948) 137.
20) S. Chikazumi: *Physics of Magnetism* (J. Wiley & Sons, New York, London and Sydney, 1964) Chap. 5.
21) A. E. Clark and E. Callen: J. appl. Phys. **39** (1964) 5972.
22) J. Bernasconi and D. Kuse: Phys. Rev. **B3** (1971) 811.
23) Results of our experiments in collaboration with the National Institute for Researches in Inorganic Materials will be published shortly.
24) M. A. Gilleo: J. Phys. Chem. Solids **13** (1960) 33.